

Static Properties of a Stacking Chain

Yu-Jane Sheng,[†] Han-Jou Lin,[†] Jeff Z. Y. Chen,[‡] and Heng-Kwong Tsao^{*,§}*Department of Chemical Engineering, National Taiwan University, Taipei, Taiwan 106, R.O.C.; Department of Physics, University of Waterloo, Waterloo, Ontario, Canada N2L 3G1; and Department of Chemical and Materials Engineering, National Central University, Jhongli, Taiwan 320, R.O.C.**Received July 7, 2004; Revised Manuscript Received September 20, 2004*

ABSTRACT: Polynucleotides are often modeled as the wormlike chain, which characterizes the local stiffness by the bending rigidity. However, some experimental findings unravel that the rigidity arises mainly from the stacking interactions between two consecutive bases along the polynucleotide. Homogeneous polynucleotides such as polydeoxyadenosines can be considered as a stacking chain, in which bases are classified either stacked or free. While a wormlike chain tends to bend evenly due to thermal fluctuations, the bending of a stacking chain requires breakage of a noncovalent chemical bond between consecutive polymer segments. The thermodynamic properties and structures of the stacking chain are investigated by Monte Carlo simulations. Analytical expressions can be obtained if the excluded-volume interaction is neglected. Fundamentally different from the wormlike chain, the crossover of the stacking chain from stiff to flexible polymer is depicted by characteristic temperatures displayed in structural and thermodynamic properties.

I. Introduction

RNA or single-stranded DNA is a linear chain formed by four different types of monomers (nucleotide bases). These polynucleotides may fold into high-order structures, similar to proteins, because of the formation of base pairs between complementary nucleotide bases, A and U (T in the case of ssDNA) and G and C. These configurations may be further stabilized by the vertical stacking interactions between adjacent base pairs. That is, base stacking is as crucial to stabilization of the secondary and tertiary structures of polynucleotides as base pairing is.¹ One experimental measure of stacking in RNA pointed out that stacking and hydrogen bonding each contribute about 1 kcal/mol per base pair to the total stability.² In fact, a single-stranded polynucleotide is able to form a stable single-stranded helix without any base pairing partners if its nucleotide bases are proficient at stacking.¹

Base stacking is characterized by an extensive overlap of the aromatic ring systems of adjacent base heterocycles and the stacking interaction involves London dispersion forces and interactions between partial charges within the adjacent rings.³ Aromatic stacking in polynucleotides takes place mainly between bases with one strand of the helix, albeit there is also a contribution of stacking between bases in opposite strands of a duplex due to the helical twist. It has been recognized for some time that the bicyclic purines (A and G) stack more strongly than do pyrimidines (C and U).^{1,2} As a result, the stacking interaction can lead to composition-sensitive rigidity of a polynucleotide.⁴

The single- and double-stranded DNA are often modeled as a semiflexible chain, which characterizes the local stiffness by the bending rigidity κ or equivalently the persistence length l_p .^{5,6} When the overall length L is large compared to the average persistence length, the physical properties are insensitive to the details of

backbone rigidity because the bending fluctuations destroy the memory of the chain direction.⁷ For example, long ssDNAs are commonly treated as highly flexible polymers with a persistent length of a few bases.^{8,9} As for relatively short polynucleotide strands, the chain stiffness is invoked to explain the chain characteristics. The typical example is the wormlike chain. The mean square of the tangent vector is identically equal to unity everywhere along a wormlike chain, and the end-to-end distance has the Kratky–Porod form¹⁰

$$\langle R^2 \rangle = 2l_p L \left\{ 1 - \frac{l_p}{L} \left[1 - \exp\left(-\frac{L}{l_p}\right) \right] \right\} \quad (1)$$

where $l_p = \kappa/k_B T$. However, recent experimental studies clearly showed the significance of base-type-dependent rigidities in the specially designed polynucleotides.^{4,11–13} For a short homogeneous ssDNA, such as poly(A) (polydeoxyadenosines) or poly(T) (polydeoxythymidines), the notation of the DNA rigidity implied in the wormlike chain becomes meaningless if the contour length is comparable to or smaller than the persistent length, i.e., Ll_p .

Those experimental findings^{4,11–13} unravel that the rigidity of single-stranded poly(A) arises primarily from the stacking interactions between two consecutive bases along the polynucleotide, as depicted in Figure 1a. This rigidity characteristic associated with base stacking is fundamentally different from the bending rigidity displayed by the wormlike chain. The disruption of base stacking in the hairpin-loop formation of ssDNA leads to sequence-dependent chain dynamics. According to the theory for coil-to-loop crossover of a flexible chain,¹⁴ the closing free energy barrier is purely entropic, and hence the closing kinetic depends only on the loop length. In ssDNA beacon experiments,⁴ poly(T) behaves essentially like a highly flexible polymer. However, poly(A) distortion requires an additional enthalpy of 0.5 kcal mol^{−1} base^{−1}, which is consistent with the disruption of base stacking. Goddard and co-workers⁴ further verify the importance of base stacking in the chain dynamics with a single cytosine defect (a different base) in the poly(A)

[†] National Taiwan University.[‡] University of Waterloo.[§] National Central University.

* Corresponding author. E-mail: hktsao@cc.ncu.edu.tw.

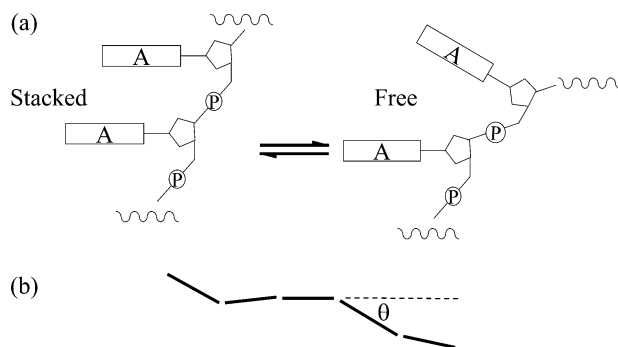


Figure 1. (a) Formation and breakage of a stacking bond between two consecutive monomers in a single polynucleotide. (b) Schematic representation of a stacking chain.

loop sequence. They find that such a defect significantly perturbs the stacking and the closing time can be twice as fast at low temperatures. For polynucleotides, the electrostatic repulsion between charged groups on the chain also contributes to the rigidity of the chain. In a low-salt limit, the electrostatic contribution l_{elec} can be as important as that due to the stacking interaction. However, in a high-salt limit (~ 0.25 M) as in aforementioned experiments,⁴ the contribution l_{elec} is estimated to be less than 1 Å and can be ignored.¹⁵

The roles of stacking interactions on the behavior of the biopolymers have been theoretically investigated from different aspects. Mansfield¹⁶ introduced a broken wormlike chain model, which incorporated abrupt breaks, or kinks, at random intervals into the original wormlike chain. Very little difference between properties of broken and regular wormlike chains was reported. Theoretical studies by Zhang et al.¹⁷ on the force/extension characteristics obtained by single-molecule manipulation techniques indicate that base-pair stacking interactions, although short-ranged in nature, dominate the elasticity of double-stranded DNA.¹⁷ The asymmetric base-stacking potential was introduced to ensure a relaxed dsDNA to take on a right-handed double-helix configuration.¹⁷ On the basis of a modified free jointed chain with vertical stacking interactions between neighboring base pairs, Zhang et al.¹⁸ also concluded that the base-pair stacking played a major role in the hairpin-coil structural transition of a ssDNA due to external stretching. Dimitrov and Zuker¹⁹ showed that including stacking between neighboring nucleotide residues of single unfolded strands in the nearest-neighbor approach improved agreement with heat capacities of melting experiments for double-stranded nucleic acids. To answer the experiments cited in ref 4, Aalberts et al.²⁰ have modeled the closing kinetics and obtained stacking enthalpies and entropies for single-stranded nucleic acids. Recently, effects of stacking on the configurations and elasticity of long homopolynucleotides are explored on the basis of straightforward modification of models for the helix-coil transition in polypeptides.^{21,22} Stacking interactions give rise to configurations of an annealed rod-coil multiblock copolymer, and a nonmonotonic dependence of size on temperature is predicted.²¹

When a wormlike chain is bent by thermal fluctuations or external forces, it tends to bend evenly. If the stacking interaction is involved, however, this physical scenario breaks down because chain bending requires breakage of a noncovalent chemical bond between consecutive polymer segments. The corresponding bending rigidity involves bond-breakage probability.¹⁵ As a

consequence, the stacking chain is fundamentally different from the wormlike chain. In this paper, we aim to investigate the influence of stacking interactions on the behavior of a linear polymer. On the basis of the characteristics associated with poly(A), we construct a stacking chain model and evaluate its thermodynamic properties and structures with/without excluded-volume interactions.

II. Stacking Chain Model

Consider a linear chain consisting of bases (segments) as shown in Figure 1a. Any two consecutive bases interact with each other via stacking interactions if they are aligned. We do not attempt to further clarify the origin of base stacking. For simplicity, we adopt a simple but physical motivated model for the stacking interaction, the two-state model.¹⁵ That is, the two segments are either stacked or free. The stacking interaction leads to an energy gain $-\epsilon_s < 0$ and therefore tends to straighten the backbone of the polymer. As schematically illustrated in Figure 1b, the angle between two neighboring segments (θ) can be used to identify whether they are stacked or not. If the angle between two consecutive segments is less than a critical angle θ_0 ($\theta < \theta_0$), the stacking bond is formed and an energy $-\epsilon_s$ is gained. Otherwise, they are free to bend. In summary, the stacking interaction between i and $i + 1$ segments ($U_{i,i+1}$) is given by

$$U_s(\theta) = \begin{cases} -\epsilon_s, & \theta < \theta_0 \\ 0, & \theta \geq \theta_0 \end{cases} \quad (2)$$

On the basis of the stacking model, eq 2, we are able to derive analytically the properties of thermodynamics and structures associated a stacking polymer without excluded-volume interactions.

When the excluded-volume interaction is considered, off-lattice Monte Carlo simulations are performed to evaluate the static properties. The simulation procedures are briefly described as follows. The details can be seen elsewhere.^{14,23} The stacking chain is modeled as a jointed hard-sphere chain with N beads of diameter σ . All the characteristic lengths are then scaled by σ . The system simulated contains a single polymer chain with chain length N ranging from 15 to 60. The bonded beads i and $i + 1$ interact via an infinitely deep square well potential²³

$$U_{i,i+1} = \begin{cases} \infty, & |\mathbf{R}_i - \mathbf{R}_{i+1}| < \sigma \\ 0, & \sigma \leq |\mathbf{R}_i - \mathbf{R}_{i+1}| < 1.2\sigma \\ \infty, & 1.2\sigma \leq |\mathbf{R}_i - \mathbf{R}_{i+1}| \end{cases}$$

At each MC step, a randomly selected bead on the chain was allowed to move around its previous position with a restriction of the bond fluctuation between σ and 1.2σ . Bond crossing (phantom chain) can be prevented by such as a choice. In addition, the stacking interaction between consecutive segments is via the simple two-state model depicted by eq 2. The temperature T^* is scaled by an energy parameter ϵ_0 , i.e., $T = k_B T^* / \epsilon_0$. Without the loss of generality, we assume the stacking energy $\epsilon_s = 5\epsilon_0$ and the critical angle $\cos \theta_0 = 0.95$. The new configurations resulting from this move are accepted according to the standard Metropolis acceptance criterion. Runs of the same length at different temperatures are equilibrated for 20 million steps. Measure-

ments for static properties are then taken over a period of 5–10 million MC steps per bead.

A. Thermodynamics. The partition function of the stacking chain with $N - 1$ segments (N beads) can be written as

$$\mathcal{Z} = \sum_{n=0}^{N-2} g(n) \exp(\beta n \epsilon_s) \quad (3)$$

where β denotes the inverse temperature $\beta = 1/k_B T^*$ and $g(n)$ represents the degeneracy associated with the state of n stacked bonds. When the excluded-volume interaction is neglected, the stacked probability between two neighboring segments is proportional to $(1 - \cos \theta_0)/2$. As a consequence, the degeneracy can be estimated by

$$g(n) = C_n^{N-2} \left(\frac{1 - \cos \theta_0}{2} \right)^n \left(\frac{1 + \cos \theta_0}{2} \right)^{N-2-n} \quad (4)$$

where $C_n^N = N!/(N - n)!n!$. Inserting eq 4 into eq 3 yields

$$\mathcal{Z} = \frac{1}{2^{N-2}} [(1 + \cos \theta_0) + (1 - \cos \theta_0) e^{\beta \epsilon_s}]^{N-2} \quad (5)$$

The Helmholtz free energy is related to the partition function by

$$\mathcal{F} = -k_B T^* \ln \mathcal{Z} = -(N - 2) k_B T^* \left\{ \ln \left[1 + \left(\frac{1 - \cos \theta_0}{1 + \cos \theta_0} \right) e^{\beta \epsilon_s} \right] + \ln \left(\frac{1 + \cos \theta_0}{2} \right) \right\} \quad (6)$$

The internal energy is equivalent to the average number of stacking interactions $\langle n \rangle$ and thus

$$\langle U \rangle = -\langle n \rangle \epsilon_s = -\left(\frac{\partial \ln \mathcal{Z}}{\partial \beta} \right) = -(N - 2) \epsilon_s \frac{p e^{\beta \epsilon_s}}{1 + p e^{\beta \epsilon_s}} \quad (7)$$

where

$$p = \left(\frac{1 - \cos \theta_0}{1 + \cos \theta_0} \right) \ll 1$$

The entropy is simply $-T^* S = \mathcal{F} - \langle U \rangle$. One can easily show that at high temperature ($\beta \epsilon_s \ll 1$) $\langle U \rangle \simeq -(N - 2) \beta \epsilon_s [(1 - \cos \theta_0)/2 + \beta \epsilon_s \sin^2 \theta_0/4]$ and $\beta \mathcal{F} \simeq -(N - 2) \beta \epsilon_s - [(1 - \cos \theta_0)/2 + \beta \epsilon_s \sin^2 \theta_0/8]$. Therefore, the entropy reduction due to stacking interactions is only $S/k_B \simeq -(N - 2)(\beta \epsilon_s)^2 \sin^2 \theta_0/8 < 0$. Here we set the free energy (or entropy) of the Gaussian chain with $(N - 1)$ segments as zero. At low temperature ($\beta \epsilon_s \gg 1$), $\langle U \rangle \simeq -(N - 2) \beta \epsilon_s$ and $\beta \mathcal{F} \simeq -(N - 2) \{ \beta \epsilon_s + \ln[(1 - \cos \theta_0)/2] \}$. Thus, the entropy reduction in comparison with a Gaussian chain is given by $S/k_B \simeq (N - 2) \ln[(1 - \cos \theta_0)/2] < 0$.

The heat capacity C_v can also be calculated by

$$\frac{C_v}{k_B} = \frac{\langle U^2 \rangle - \langle U \rangle^2}{(k_B T^*)^2} = -\beta^2 \frac{\partial \langle U \rangle}{\partial \beta} = (N - 2)(\beta \epsilon_s)^2 \frac{p e^{\beta \epsilon_s}}{[1 + p e^{\beta \epsilon_s}]^2} \quad (8)$$

Note that $C_v \rightarrow \beta^2$ as $\beta \rightarrow 0$ and $C_v \rightarrow \beta^2 e^{-\beta \epsilon_s}$ as $\beta \rightarrow \infty$.

Therefore, there must exist a characteristic temperature T_c (β_c) so that $(\partial C_v / \partial T) = 0$. At this temperature, the extent of the internal energy fluctuation is maximum. It depicts a crossover temperature. Below T_c , the stacking chain behaves like a stiff polymer while it is more like a random coil as $T > T_c$.

B. Structure. The size of the stacking polymer can be characterized by the mean square end-to-end distance. The end-to-end vector of the chain is defined as

$$\mathbf{R} = \mathbf{R}_N - \mathbf{R}_1 = \sum_{i=1}^{N-1} \mathbf{r}_i \quad (9)$$

where the bond vector \mathbf{r}_i is related to the bead position \mathbf{R}_j by $\mathbf{r}_i = \mathbf{R}_{i+1} - \mathbf{R}_i$. The mean square end-to-end distance is then given by

$$\begin{aligned} \langle \mathbf{R}^2 \rangle &= \sum_{i=1}^{N-1} \sum_{j=1}^{N-1} \langle \mathbf{r}_i \cdot \mathbf{r}_j \rangle \\ &= \sum_{i=1}^{N-1} \langle \mathbf{r}_i^2 \rangle + 2 \sum_{i=1}^{N-1} \sum_{k=1}^{N-1-i} \langle \mathbf{r}_i \cdot \mathbf{r}_{i+k} \rangle \end{aligned} \quad (10)$$

Similar to the general random flight models,¹⁰ $\langle \mathbf{r}_i \cdot \mathbf{r}_{i+k} \rangle$ does not vanish and can be calculated. The average of \mathbf{r}_{i+k} is taken with the rest of the chain fixed

$$\langle \mathbf{r}_{i+k} \rangle_{\mathbf{r}_1, \dots, \mathbf{r}_{i+k-1}} = \mathbf{r}_{i+k-1} \alpha \quad (11)$$

where α denotes the average of $\cos \theta$

$$\alpha = \langle \cos \theta \rangle = \frac{1}{2} (1 + \cos \theta_0) \left[\frac{1 - e^{-\beta \epsilon_s}}{1 + p^{-1} e^{-\beta \epsilon_s}} \right] \quad (12)$$

Note that $\alpha \rightarrow 0$ as $\beta \epsilon_s \rightarrow 0$ and $\alpha \rightarrow 1/2(1 + \cos \theta_0)$ as $\beta \epsilon_s \gg 1$. Multiplying both sides of eq 11 by \mathbf{r}_i and taking the average over $\mathbf{r}_i, \dots, \mathbf{r}_{i+k-1}$, one has

$$\langle \mathbf{r}_i \cdot \mathbf{r}_{i+k} \rangle = \alpha \langle \mathbf{r}_i \cdot \mathbf{r}_{i+k-1} \rangle \quad (13)$$

The recursion relation, with the initial condition $\langle \mathbf{r}_i^2 \rangle = b^2$, is solved by

$$\langle \mathbf{r}_i \cdot \mathbf{r}_{i+k} \rangle = b^2 \alpha^k \quad (14)$$

The mean square segment length is $b^2 = 3(l_2^5 - l_1^5)/5(l_2^3 - l_1^3)$ if the segment length l fluctuates from l_1 to l_2 ($l_1 \leq l \leq l_2$). In the present study, b is related to the bead diameter by $b \simeq 1.1\sigma$. Using eq 14 in eq 10, the mean square end-to-end distance is given by

$$\langle \mathbf{R}^2 \rangle = (N - 1) b^2 \frac{1 + \alpha}{1 - \alpha} \left[1 - \frac{2}{N - 1} \alpha \frac{1 - \alpha^{N-1}}{1 - \alpha^2} \right] \quad (15)$$

For large N , $\langle \mathbf{R}^2 \rangle = (N - 1) b^2 [(1 + \alpha)/(1 - \alpha)]$. Similarly, results have been obtained by the correlated random walk model.²⁴

The persistent length is another fundamental feature of the stacking chain. The concept of persistent length is a measure of stiffness. However, there are several definitions. We consider the projection length l_p and the orientation correlation length l .²⁵ The latter is defined as the correlation length of an orientational correlation

function with an exponential decay. It can be easily obtained from eq 14

$$\langle \cos \theta_{i,i+k} \rangle = \alpha^k = e^{-kb/l}, \text{ if } b \ll l \quad (16)$$

As a result, the persistent length is given by

$$l = -\frac{b}{\ln \alpha} \quad (17)$$

As the temperature declines, the persistent length is increased and approaches $l \rightarrow -b/\ln[(1 + \cos \theta_0)/2]$.

The projection length is defined as the projection of the end-to-end vector on the direction of the first bond

$$l_p = \frac{1}{b} \langle \mathbf{r}_1 \cdot \mathbf{R} \rangle \quad (18)$$

Inserting eq 9 into eq 18 and using eq 14 yields

$$l_p = \frac{1}{b} \sum_{j=1}^{N-1} \langle \mathbf{r}_1 \cdot \mathbf{r}_j \rangle = b \frac{1 - \alpha^{N-1}}{1 - \alpha} \quad (19)$$

For large N

$$\frac{l_p}{b} = \frac{1}{1 - \alpha} \quad (20)$$

When $\cos \theta_0 \ll 1$ ($p \ll 1$) and $\beta\epsilon_s \gg 1$, eq 17 reduces to eq 20, and both definitions are equivalent. In the temperature range $e^{-\beta\epsilon_s} \gg p$, $\alpha \approx p \exp(\beta\epsilon_s)$ and the persistent length varies with the temperature according to $l_p/b \approx 1 + p \exp(\beta\epsilon_s)$. When $p \gg e^{-\beta\epsilon_s}$, $\alpha \approx 1 - \exp(-\beta\epsilon_s)$ and the persistent length grows exponentially, $l_p/b \approx \exp(\beta\epsilon_s)$. This is in contrast to $l_p \sim \beta$ in the conventional wormlike chain model, as will be discussed in the following section. When $\beta\epsilon_s \ll 1$, however, $l_p \rightarrow b$ but $l \rightarrow 0$ because l is corresponding to a continuous chain with $l \gg b$.

III. Results and Discussion

The rigidity of single-stranded polynucleotides is mainly determined by the stacking interactions between two consecutive bases along the strand. This leads to sequence-dependent looping kinetics, intrinsically different from that of a wormlike chain.⁴ In this paper we introduce a simple but physically motivated model to describe the stacking-induced stiffness of a polymer. When the excluded-volume interaction is neglected, the static properties of a stacking chain can be derived analytically. Monte Carlo simulations are performed to calculate the static properties as volume interactions are considered. The crossover behavior from flexible to stiff chain can be evidently seen on the basis of those static properties. The comparison between the wormlike chain and the stacking chain are then made to demonstrate their fundamental differences.

A. Structural Properties. The structural properties change with the temperature, and the crossover from flexible to stiff polymers can be clearly demonstrated through end-to-end distance, radius of gyration, and structure factor. Figure 2 depicts the variation of the end-to-end distance with the temperature with and without excluded-volume interactions for different chain length. At low temperature (large $\beta\epsilon_s$), the stacking interactions tend to straighten the chain and lead to large end-to-end distance. On the other hand, at high

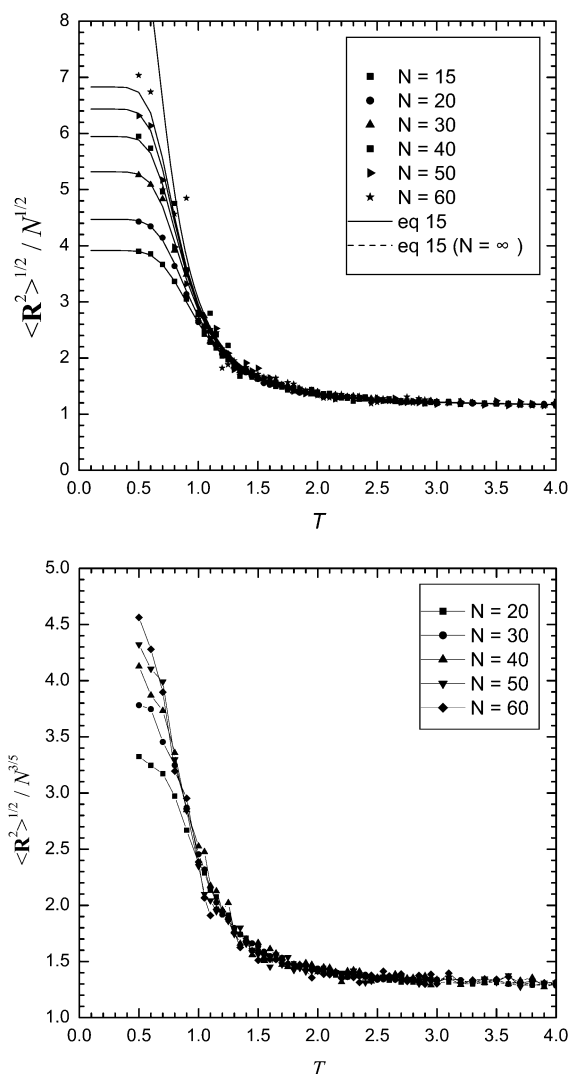


Figure 2. Variation of the end-to-end distance with the temperature for different chain lengths (a) without and (b) with excluded-volume interactions.

temperature, the thermal energy dominates over the stacking energy, and thereby the polymer displays the behavior similar to an ideal chain or a hard-sphere chain. As shown in Figure 2a for stacking chains without volume interactions, $\langle R^2 \rangle^{1/2}$ scaled with $N^{1/2}$ for different chain lengths collapse into a single curve at high enough temperature. The Monte Carlo results agree quite well with the theoretical expression, eq 15. Similar behavior is observed for stacking chains with volume interactions, as depicted in Figure 2b. Note that $\langle R^2 \rangle^{1/2}$ is scaled with $N^{3/5}$, which is the length scale associated with the hard-sphere chain. Our results show a monotonic dependence of size on temperature, which disagrees with the prediction based on the modified Zimm–Bragg model with the difference between the monomer size in the stacked, helical state, and random-coil configuration.²¹

In general, the radius gyration $\langle R_g^2 \rangle$ is proportional to the end-to-end distance $\langle R^2 \rangle$, and hence the effect of chain length is canceled out in the ratio of the two length scales. As a consequence, a plot of $\langle R_g^2 \rangle^{1/2} / \langle R^2 \rangle^{1/2}$ against temperature should yield a single curve for different chain lengths, as shown in Figure 3. The length ratio declines with decreasing temperature. At high temperature, the ratio for the polymer without volume

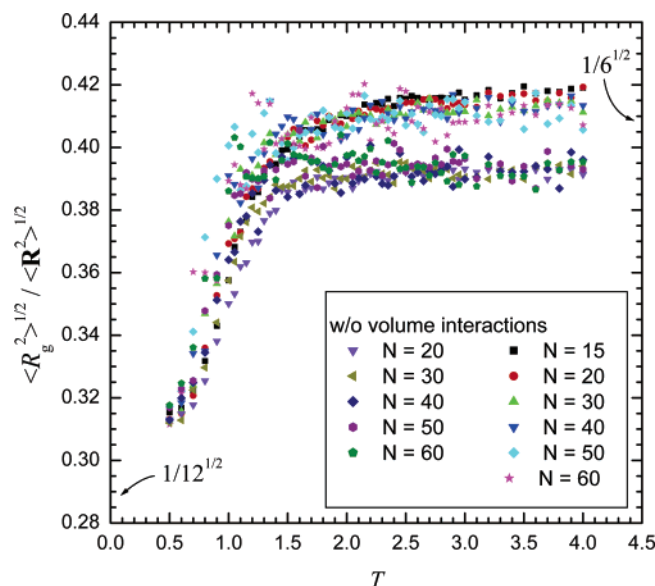


Figure 3. Length ratio of radius of gyration to end-to-end distance is plotted against the temperature for different chain lengths of a stacking polymer with and without volume interactions.

interactions is about $1/\sqrt{6}$, the Gaussian chain limit. On the contrary, at low temperature, the ratio approaches the rigid-rod limit, $1/\sqrt{12}$. For the chain with volume interactions, $\langle R_g^2 \rangle^{1/2} / \langle R^2 \rangle^{1/2}$ at high temperature is about 0.39, slightly less than the Gaussian chain limit. Although there exists quantitative differences between the stacking chains with and without excluded-volume interactions, both types do display qualitatively similar behavior.

The structural characteristics associated with a single chain can be illustrated through the static structure factor, which is calculated by¹⁰

$$S(q) = \left\langle \frac{\sin \mathbf{q} \cdot (\mathbf{R}_i - \mathbf{R}_j)}{\mathbf{q} \cdot (\mathbf{R}_i - \mathbf{R}_j)} \right\rangle$$

where \mathbf{q} denotes the scattering vector and $q = |\mathbf{q}|$. For $qR_g \ll 1$, the expansion of $S(q)$ yields

$$S(q) \approx 1 - \frac{1}{3}(qR_g)^2 + \dots \quad (21)$$

On the other hand, the scaling analysis¹⁰ indicates that $S(q)$ is independent of N if $qR_g \gg 1$

$$S(q) \sim (qR_g)^{-1/\nu} \quad (22)$$

where ν is the exponent in $\langle R^2 \rangle^{1/2} \propto N^\nu$. Figure 4a depicts the variation of the structure factor with qR_g for a stacking chain with $N = 30$. At relative high temperature the stacking energy can be overcome by the thermal energy, and $S(q)$ behaves close to an ideal chain ($\nu = 1/2$, without volume interactions) or a hard-sphere chain ($\nu \approx 3/5$ with volume interactions). On the contrary, at low enough temperature the stacking interaction dominates over the thermal energy, and $S(q)$ displays a rodlike feature ($\nu = 1$) with and without excluded-volume interactions. Because the polymer structure changes with the temperature gradually, it is expected that ν rises from about $3/5$ to 1.0 as T is decreased. Consequently, one is able to extract the exponent $\nu(T)$

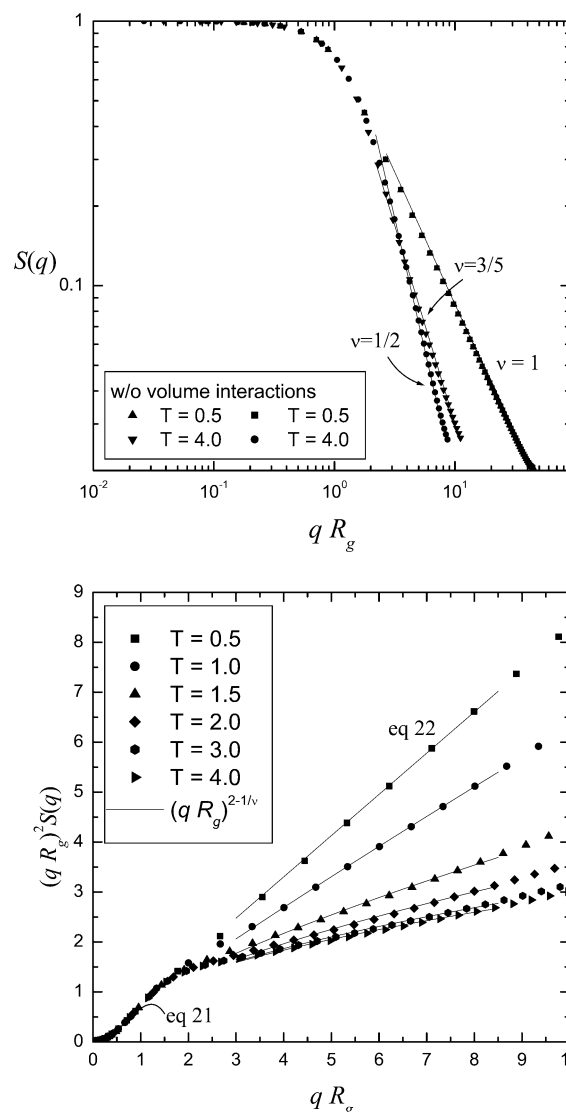


Figure 4. (a) Variation of the static structure factor with qR_g at $T = 0.5$ and 4.0 for $N = 30$. (b) Kratky plot at different temperatures for a stacking chain with volume interactions.

from the Kratky form, i.e., $(qR_g)^2 S(q)$ vs qR_g . Figure 4b shows that the Kratky plot follows eq 21 for small qR_g and eq 22 for relative large qR_g . The exponents are $\nu \approx 0.66, 0.68, 0.72, 0.77, 0.93$, and 1.0 for $T = 4.0, 3.0, 2.0, 1.5, 1.0$, and 0.5 , respectively. This consequence confirms that the stacking chain varies from a random coil to a stiff chain with decreasing temperature.

B. Comparison between a Wormlike Chain and a Stacking Chain. It is worth comparing the behavior of a stacking chain with that of a discrete wormlike chain. Consider a linear chain with the bending energy between two consecutive segments, then the total bending energy is²⁶

$$U_b = \frac{\kappa}{2} \sum_{i=1}^{N-2} (\mathbf{u}_{i+1} - \mathbf{u}_i)^2 = \kappa \sum_{i=1}^{N-2} (1 - \cos \theta_i) \quad (23)$$

where \mathbf{u}_i is the unit vector directing from bead i to bead $i + 1$ and $\cos \theta_i = \mathbf{u}_i \cdot \mathbf{u}_{i+1}$. The parameter κ represents the local bending energy that controls the rigidity of the chain. Note that the above equation is simply the discrete realization of a continuous wormlike chain.

When the volume interaction is neglected, the partition function is given by

$$\mathcal{Z}_b = \frac{1}{(N-2)!} \prod_{i=1}^{N-2} \int_0^\pi \exp[-\beta U_b(\theta_i)] \sin \theta_i d\theta_i \quad (24)$$

On the basis of eq 24, the internal energy and the heat capacity can be calculated

$$\beta \langle U \rangle = (N-2)[1 + \beta \kappa(1 - \coth \beta \kappa)] \quad (25)$$

and

$$\frac{C_v}{k_B} = (N-2)[1 + (\beta \kappa)^2(1 - \coth^2 \beta \kappa)] \quad (26)$$

When $\beta \kappa$ is increased, the internal energy is monotonically increased and the heat capacity displays an inflection point. Compared to the stacking chain, the characteristic temperature associated with the crossover from flexible to stiff polymer is absent on the basis of the thermodynamic properties.

The structural properties of a discrete wormlike chain can also be represented by eq 15 for mean square end-to-end distance and by eq 17 for the persistent length. The parameter $\alpha = \langle \cos \theta \rangle$ is given by

$$\alpha = \frac{\int_0^\pi \exp[-\beta \kappa(1 - \cos \theta)] \cos \theta \sin \theta d\theta}{\int_0^\pi \exp[-\beta \kappa(1 - \cos \theta)] \sin \theta d\theta} = \coth \beta \kappa - \frac{1}{\beta \kappa} \quad (27)$$

where $\alpha \approx \beta \kappa/3$ as $\beta \kappa \ll 1$ and $\alpha \approx 1 - (\beta \kappa)^{-1}$ as $\beta \kappa \gg 1$. The continuous limit in eq 16, $b/l \rightarrow 0$, corresponds to

$$\alpha = \exp(-b/l) \approx 1 - b/l$$

Substituting the above result into eq 15 recovers the Kratky–Porod form, eq 1, with $L = (N-1)b$. When $\beta \kappa$ is large enough to ensure $b/l \ll 1$, comparing the above results also gives the relation between the persistent length and the temperature

$$\frac{l}{b} \approx \beta \kappa \quad (28)$$

which is consistent with that of a continuous wormlike chain. Inserting eq 27 into eqs 15 and 17 for large N shows monotonic increases in both $\langle R^2 \rangle$ and l with increasing β . It should be emphasized that the energy cost for bending depends on the radius of curvature in a wormlike chain but on the number of stacking bonds broken in a stacking chain. The persistent length of the stacking chain varies inversely with the probability of breaking base stacking: $l_p \sim \exp(\epsilon_s/k_B T)$, which is in contrast to $l \sim \kappa/k_B T$ in a wormlike chain. Therefore, the behavior of the stacking chain is fundamentally different from that associated with the wormlike chain.

C. Crossover Temperature. The pronounced feature of a stacking chain is the crossover temperature T_c , which characterizes the crossover from a stiff chain to a random coil. Both thermodynamic and structural properties display such a crossover behavior. Nevertheless, the crossover temperature may vary with the definition. Figure 5 shows the variation of the breakage probability of the stacking interaction (equivalent to the

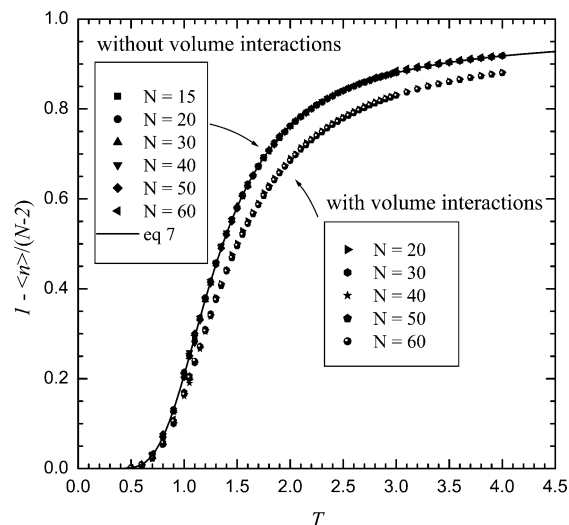


Figure 5. Variation of the unstacking probability (related to the internal energy) with the temperature for different chain lengths of a stacking chain with and without volume interactions.

internal energy) with the temperature for different chain lengths with and without excluded-volume interactions. The MC results of the latter can be well represented by the theoretical expression, eq 7. With increasing T , the breakage probability approaches $(1 + \cos \theta_0)/2$ asymptotically, which simply reflects the probability in the stacking free region due to random orientation. Similar behavior is observed for polymers with volume interactions. Nonetheless, as shown in Figure 5, the hard-sphere interaction tends to expand the coil and thereby favors the stacking bond formation. In such a probability curve, the crossover temperature T_c can be identified as the temperature at which $\langle n \rangle / (N-2) = 1/2$ or $\partial^2 \langle U \rangle / \partial T^2 = 0$. According to eq 7, the crossover temperature is simply

$$k_B T_c = \frac{\epsilon_s}{\ln p^{-1}} \quad (29)$$

The crossover nature can also be exhibited through the internal energy fluctuation. Figure 6 demonstrates the variation of the heat capacity with the temperature for different chain lengths with and without volume interactions. A peak is observed, and the heat capacity curve with volume interactions can be well represented by eq 8. At low temperature, the chain is nearly straight, and thus the behavior of C_v is essentially the same for a stacking chain with and without volume interactions. When the temperature is high enough, however, the energy fluctuation associated with taking into account the volume interaction is more significant because the space for the stacking-free state is less available. Nevertheless, the peaks of both cases occur at almost the same temperature. In accordance with the heat capacity curve, the crossover temperature can be defined as the peak temperature

$$\frac{\partial C_v}{\partial T} = 0 = (\beta_c \epsilon_s + 2)e^{-\beta_c \epsilon_s} - p(\beta_c \epsilon_s - 2) \quad (30)$$

or

$$\beta_c \epsilon_s \approx \ln p^{-1} + \ln \frac{\ln p^{-1} + 2}{\ln p^{-1} - 2} \quad (31)$$

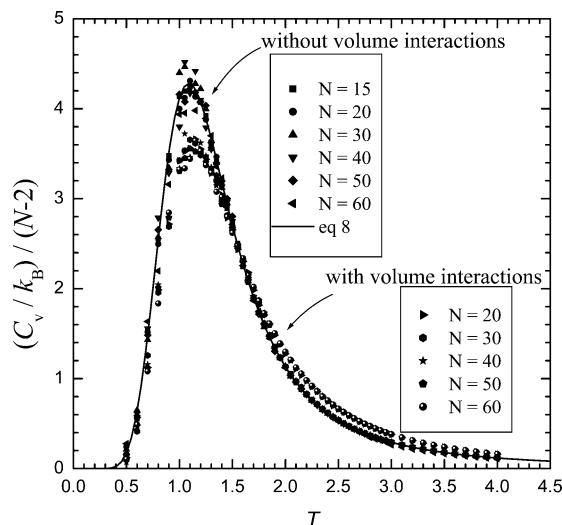


Figure 6. Variation of the heat capacity with the temperature for different chain lengths of a stacking chain with and without volume interactions.

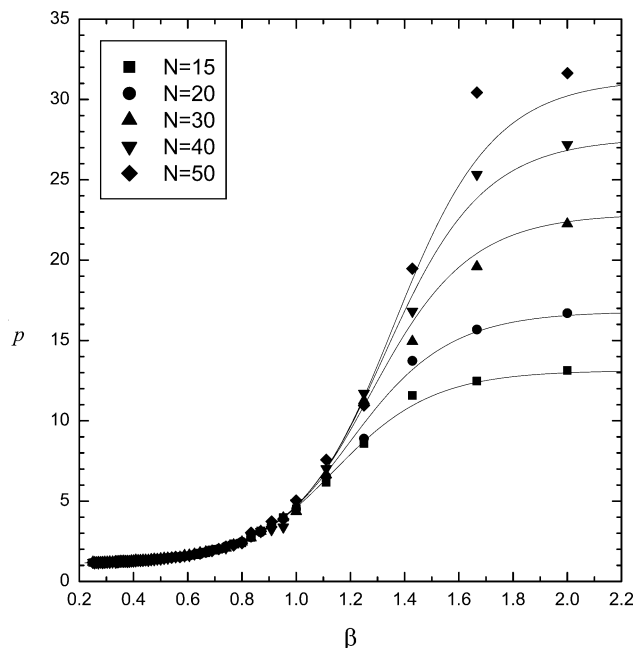


Figure 7. Plot of the persistent length against the temperature for different chain lengths of a stacking chain without volume interactions.

Evidently, the crossover temperatures are essentially the same for definitions based on heat capacity and internal energy when $p^{-1} \gg 1$ or $(1 - \cos \theta_0) \ll 1$.

Similarly to the thermodynamic properties, the crossover temperature can also be defined by the structural properties. Figure 7 depicts the variation of the persistent length l_p with the temperature. The persistent length calculated by MC agrees quite well with the theoretical expression, eq 19. At low temperature, the persistent length for $\alpha^N \ll 1$ approaches $2b/(1 - \cos \theta_0)$ asymptotically. In other words, the upper limit of the persistent length is about 44σ if $\cos \theta_0 = 0.95$. We can define the crossover temperature T_c' as the point of $\partial^2 \langle R^2 \rangle / \partial^2 \beta = 0$ or $\partial^2 l_p / \partial^2 \beta = 0$. Using eq 15 or 20 and assuming $p^{-1} e^{-\beta \epsilon_s} \ll 1$ yields

$$\beta' \epsilon_s \approx 2 \ln p^{-1} + p \frac{1 - \cos \theta_0}{2} \quad (32)$$

The assumption is justified if $p \ll 1$. The above results show that the crossover temperature is determined by the stacking energy and the critical angle. The latter reflects the entropy associated with the stacked bond (available space for stacking bond fluctuation). When the critical angle approaches zero, the thermal fluctuation in the stacked-free space comes to dominate over the stacking energy gain, and the random coil is preferred rather than the stiff chain. Thereby, the crossover occurs at temperatures close to zero. It is interesting to find that the crossover temperature based on the thermodynamic property is twice that based on the structural property, i.e., $T_c = 2T_c'$ if $p \ll 1$. This consequence indicates that the crossover of thermodynamic properties always takes place at higher temperature than that associated with structural properties.

In our stacking chain model, both the bases and sugars are absorbed in the coarse-grained segment. The stacking interaction between the bases, which in reality are side groups that stick out from the linear backbone of the polymer, is effectively accounted for via an polar angle-dependent potential. In reality, destacking could also occur at a fixed bond angle via a rotation about the azimuthal angle. Most of the previous work simply adopted vertical stacking interactions between neighboring base pairs in the nearest-neighbor approximation.^{18–21} The microscopic detail was not considered. Although we adopt local cylindrical symmetry assumption for the stacking interaction, our model grasps the essential feature of a stacking chain. Introducing azimuthal angle dependence is straightforward and will not affect the qualitative behavior of the stacking chain. In addition, those large residues would have an impact on the effective Kuhn length, which can be studied by atomistic models. In this paper, however, we focus on the same coarse-grained level as the wormlike chain. As a consequence, the effect of large residues is simply taken into account by the excluded-volume interaction between segments. Our MC results indicate that the qualitative behavior of the stacking chain with/without excluded-volume interactions is similar.

We have investigated the static properties of a linear polymer whose stiffness is primarily contributed by the stacking interaction between consecutive segments. A simple but physical motivated model for the stacking interaction is proposed. The behavior of the stacking chain is fundamentally different from the wormlike chain. The persistent length of the former varies with the temperature by $l_p \propto \exp(\epsilon_s/k_B T)$, but the persistent length of the latter follows $l_p \propto \kappa/k_B T$. Moreover, the crossover happening in the stiff-to-flexible chain can be characterized by the crossover temperature for the stacking polymer. However, it is absent in the wormlike polymer. The crossover temperature is proportional to the stacking energy, which depends on the solvent environment. A typical stacking energy for AA pairs is about 10 kJ/mol.^{27,28} The crossover temperature depends also on the critical angle, which can be determined from experiments such as internal energy measurement. If one adopts $\cos \theta_0 = 0.95$, then the crossover temperature based on structural properties is roughly 250 K and that based on thermodynamic properties is about 390 K. As a consequence, such a stacking chain in the temperature range for an aqueous solution happens to be in the stiff-to-flexible crossover regime and therefore is sensitive to the change in temperature.

Acknowledgment. Y.-J.S. and H.-K.T. thank National Council of Science of Taiwan for financial support. Computing time, provided by the Nation Center for High-Performance Computing of Taiwan, is gratefully acknowledged.

References and Notes

- (1) Kool, E. T. *Chem. Rev.* **1997**, *97*, 1473.
- (2) Freier, S. M.; Sugimoto, N.; Sinclair, A.; Alkema, D.; Nielson, T.; Kierzek, R.; Caruthers, M. H.; Turner, D. H. *Biochemistry* **1986**, *25*, 3214.
- (3) Šponer, J.; Leszczyński, J.; Hobza, P. *J. Phys. Chem.* **1996**, *100*, 5590.
- (4) Goddard, N. L.; Bonnet, G.; Krichevsky, O.; Libchaber, A. *Phys. Rev. Lett.* **2001**, *85*, 2400.
- (5) Chirico, G.; Langowski, J. *Macromolecules* **1992**, *25*, 769.
- (6) Allison, S. A.; Austin, R.; Hogan, M. *J. Chem. Phys.* **1989**, *90*, 3843.
- (7) Grosberg, A. Y.; Khokhlov, A. R. *Statistical Physics of Macromolecules*; AIP Press: Woodbury, NY, 1994; Chapter 1.
- (8) Tinland, B.; Pluen, A.; Sturm, J.; Weill, G. *Macromolecules* **1997**, *30*, 5763.
- (9) Smith, S. B.; Cui, Y.; Bustamante, C. *Science* **1996**, *271*, 795.
- (10) Doi, M.; Edwards, S. F. *The Theory of Polymer Dynamics*; Oxford University Press: Oxford, 1986; Chapter 8.
- (11) Bonnet, G.; Krichevsky, O.; Libchaber, A. *Proc. Natl. Acad. Sci. U.S.A.* **1998**, *95*, 8602.
- (12) Ansari, A.; Kuznetsov, S. V.; Shen, Y. *Proc. Natl. Acad. Sci. U.S.A.* **2001**, *98*, 7771.
- (13) Wallace, M. I.; Ying, L.; Balasubramanian, S.; Klennerman, D. *Proc. Natl. Acad. Sci. U.S.A.* **2001**, *98*, 5584.
- (14) Sheng, Y.-J.; Chen, J. Z. Y.; Tsao, H.-K. *Macromolecules* **2002**, *35*, 9624.
- (15) Sain, A.; Ha, B.-Y.; Tsao, H.-K.; Chen, J. Z. Y. *Phys. Rev. E* **2004**, *69*, 061913.
- (16) Mansfield, M. L. *Macromolecules* **1986**, *19*, 854.
- (17) Zhou, H.; Zhang, Y.; Ou-Yang, Z.-C. *Phys. Rev. Lett.* **1999**, *82*, 4560. Zhou, H.; Zhang, Y.; Ou-Yang, Z. *Phys. Rev. E* **2000**, *62*, 1045.
- (18) Zhou, H.; Zhang, Y. *J. Chem. Phys.* **2001**, *114*, 8694. Zhou, H.; Zhang, Y.; Zhou, H.; Ou-Yang, Z.-C. *Biophys. J.* **2001**, *81*, 1133.
- (19) Dimitrov, R. A.; Zuker, M. *Biophys. J.* **2004**, *87*, 215.
- (20) Aalberts, D. P.; Parman, J. M.; Goddard, N. L. *Biophys. J.* **2003**, *84*, 3212.
- (21) Buhot, A.; Halperin, A. *Phys. Rev. E* **2004**, *70*, 020902(R).
- (22) Buhot, A.; Halperin, A. *Macromolecules* **2002**, *35*, 3238.
- (23) Sheng, Y.-J.; Jiang, S.; Tsao, H.-K. *Macromolecules* **2002**, *35*, 7865. Tsao, H.-K.; Chen, J. Z. Y.; Sheng, Y.-J. *Macromolecules* **2003**, *36*, 5863.
- (24) Fujita, S.; Okamura, Y.; Chen, J. T. *J. Chem. Phys.* **1980**, *72*, 3993.
- (25) Ullner, M.; Woodward, C. E. *Macromolecules* **2002**, *35*, 1437.
- (26) Chen, J. Z. Y.; Tsao, H.-K.; Sheng, Y.-J. *Europhys. Lett.* **2004**, *65*, 407.
- (27) Deweyand, T. G.; Turner, D. H. *Biopolymers* **1979**, *18*, 5757.
- (28) Luo, R.; Gilson, H. S. R.; Potter, M. J.; Gilson, M. K. *Biophys. J.* **2001**, *80*, 140.

MA0486290